Journal of Alloys and Compounds 790 (2019) 633–639

Contents lists available at ScienceDirect

Journal of Alloys and Compounds

journal homepage: http://www.elsevier.com/locate/jalcom

$Gd_{25}RE_{25}Co_{25}Al_{25}$ (RE = Tb, Dy and Ho) high-entropy glassy alloys with distinct spin-glass behavior and good magnetocaloric effect

Lin Xue [a], Liliang Shao [a], Qiang Luo [a], Baolong Shen [a, b, *]

[a] School of Materials Science and Engineering, Jiangsu Key Laboratory of Advanced Metallic Materials, Southeast University, Nanjing 211189, China
[b] Institute of Massive Amorphous Metal Science, China University of Mining and Technology, Xuzhou 221116, China

ARTICLE INFO

Article history:
Received 28 January 2019
Received in revised form
12 March 2019
Accepted 13 March 2019
Available online 16 March 2019

Keywords:
High-entropy glassy alloy
Spin-glass like behavior
Magnetocaloric effect

ABSTRACT

With different rare earth substitution, equal-atomic $Gd_{25}RE_{25}Co_{25}Al_{25}$ (RE = Tb, Dy and Ho) high-entropy glassy alloys were studied in this work. The Curie temperature of the alloy system can be easily tuned from 50 to 73 K with different rare earth substitution, which is corresponding to the change of de Gennes factor. A distinct spin-glass like behavior due to the strong random magnetic anisotropy and exchange frustration below the Curie temperature in each alloy is observed and discussed. The high-entropy glassy alloys exhibit large magnetocaloric effect. Under a magnetic field change of 5 T, the maximum of magnetic entropy change and refrigerant capacity for $Gd_{25}Ho_{25}Co_{25}Al_{25}$ glassy alloy are 9.78 J $kg^{-1}K^{-1}$ and 626 J kg^{-1}, respectively. The large magnetocaloric effect makes these high-entropy glassy alloys promising candidates as magnetic refrigerants.

1. Introduction

Compared with conventional gas refrigerants, magnetic refrigerants based on the materials with distinct magnetocaloric effect (MCE) become more attractive for refrigeration applications, due to their advantages of both high efficiency and environmental friendliness [1–5]. The MCE of a refrigerant can be mainly evaluated by the magnetic entropy change (ΔS_M) caused by the alignment of magnetic spins as the external magnetic field is applied [3], and great efforts have been devoted to increase the ΔS_M of magnetic refrigerants [6–8]. In the past decade, increasing attention has been paid to the heavy rare earth (RE) based glassy alloys exhibiting large MCE and profuse magnetic structures [6,9–11]. A number of RE (e.g. Gd, Tb, Dy, Ho and Er)-based glassy alloys showing ferromagnetic-paramagnetic transition and spin-glass (SG) like behavior have been developed [12–16], such as $Dy_{46}Y_{10}Al_{24}Co_{20}$ [12], and $Tb_{36}RE_{20}Al_{24}Co_{20}$ (RE = Gd, Ho, Er, Y, Pr, Sm) [13] glassy alloys. And the effects of constituent, microstructure and crystallization on the MCE have been extensively explored [14–17].

In recent years, novel high-entropy (HE) alloys containing multiple principal elements with equal-atomic ratio were developed, which exhibit high configuration entropy (i.e., the entropy of mixing in terms of atomic configuration, and can be expressed as ΔS_{config} = RlnN, where R is the gas constant and N is the number of constituent elements) [18,19]. It was noted that multi-principal-elemental mixtures of HE alloys result in high entropy, sluggish diffusion, lattice distortion and cocktail effects [18], and HE alloys have attracted increasing attentions in both fundamental sciences and promising applications [20–23]. For instance, $Fe_{20}Cr_{20}Mn_{20}Ni_{20}Co_{20}$ HE alloy exhibited high strength and high work-hardening rate caused by its multiple deformation modes [22], the $Ti_{25}Zr_{25}Hf_{25}Nb_{25}$ HE alloy showed improved wear resistance and lower coefficient of friction as compared to its traditional alloy counterparts [23]. In addition, $Gd_{20}Dy_{20}Er_{20}Ho_{20}Tb_{20}$ [24] and $Gd_{20}Tb_{20}Dy_{20}Al_{20}M_{20}$ (M = Fe, Co, Ni) [15] HE glassy alloys were reported to exhibit excellent MCE. And in our previous work, pentabasic $Er_{20}Dy_{20}Co_{20}Al_{20}RE_{20}$ (RE = Gd, Tb and Tm) HE glassy alloys were developed and exhibited distinct SG like behavior and large MCE [10]. Nevertheless, how atomic and magnetic structures, and the ΔS_{config} affect the MCE in HE alloys, and the nature of SG like behavior are still unclear. In order to improve the MCE and understand the spin dynamic of the HE glassy alloys, as well as decrease the RE content in the reported HE alloys, quaternary $Gd_{25}RE_{25}Co_{25}Al_{25}$ (RE = Tb, Dy and Ho) HE glassy alloys were designed and prepared in this work. And the influences of RE elements on the magnetic behavior and MCE were systematically investigated and discussed.

* Corresponding author. School of Materials Science and Engineering, Jiangsu Key Laboratory of Advanced Metallic Materials, Southeast University, Nanjing 211189, China.
E-mail address: blshen@seu.edu.cn (B. Shen).

https://doi.org/10.1016/j.jallcom.2019.03.210
0925-8388/

2. Experimental

Ingots with nominal compositions of $Gd_{25}RE_{25}Co_{25}Al_{25}$ (RE = Tb, Dy, and Ho) were prepared by arc melting pure elements (above 99.9 wt %) in an argon atmosphere. To ensure homogeneous, every ingot was remelted five times. Glassy ribbons with approximate width of 2 mm and thickness of 40 μm were prepared by single roller melt spinning method. The amorphous nature of melt-spun ribbons was certified by X-ray diffraction (XRD) with a Cu Kα radiation, and thermal analysis was performed by a differential scanning calorimeter (DSC) with a heating rate of 40 K/min. Temperature and field dependences of the DC magnetization were measured using a SQUID magnetometer (MPMS, Quantum Design). Field cooling magnetization (M_{FC}) of the ribbons was measured on the heating course after initial cooling from 300 to 2 K, with an applied magnetic field of 200 Oe through the whole process. On the other hand, the zero field cooling magnetization (M_{ZFC}) was measured on the heating course under an applied magnetic field of 200 Oe after initial cooling the sample from 300 to 2 K with zero field. Isothermal magnetization (*M-H*) curves were measured with a varying magnetic field increasing from 0 to 5 T at different temperatures ranging from 10 to 130 K. AC susceptibility was measured at frequencies ranging from 13 to 9673 Hz with DC background field of 5 Oe using a physical properties measurement system (PPMS 6000, Quantum Design).

3. Results and discussion

Fig. 1 shows the DSC curves and XRD patterns of $Gd_{25}RE_{25}Co_{25}Al_{25}$ (RE = Tb, Dy, Ho) melt-spun ribbons. As shown in the inset of Fig. 1, only broad humps without sharp crystalline peak can be observed for each pattern, verifying the amorphous structure of the ribbons. Since the growth and even nucleation of crystalline phases are gradually inhibited for the sluggish diffusion in the HE alloys [18], HE glassy alloys with single amorphous structure were easily obtained in this work. Distinct endothermic reaction due to glass transition and sharp exothermic peak related to crystallization can be observed in the DSC traces of the $Gd_{25}RE_{25}Co_{25}Al_{25}$ (RE = Tb, Dy, Ho) glassy alloys, which further confirms their fully glassy structure. The values of glass transition temperature (T_g), crystallization temperature (T_x) and the supercooled liquid region ($\Delta T_x = T_x - T_g$) obtained from the DSC curves are listed in Table 1. The high T_g above 600 K indicates a high thermal stability in the glassy alloys attributed to the high entropy effect. As the substitute element varies from Tb to Ho, the T_g and T_x increase gradually from 612 to 633 K, and 659 to 675 K, respectively, leading to an improvement of the thermal stability of the glassy alloys. Besides, for each alloy, the ΔT_x is over 40 K, indicating a high thermal stability of the supercooled liquid as well.

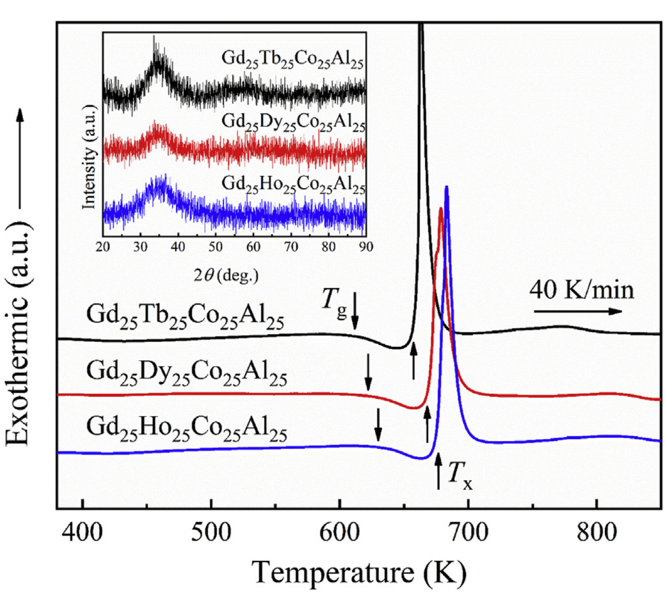

Fig. 1. XRD patterns and DSC curves of the $Gd_{25}RE_{25}Co_{25}Al_{25}$ (RE = Tb, Dy, Ho) melt-spun ribbons.

Temperature dependence of M_{FC} and M_{ZFC} for $Gd_{25}RE_{25}Co_{25}Al_{25}$ (RE = Tb, Dy, Ho) glassy alloys are shown in Fig. 2. The magnetization of the M_{FC} branches decreases and tends to zero with the increase of temperature, displaying obvious magnetic phase transition from ferromagnetic to paramagnetic state in the glassy alloys. It can be seen that magnetization increases substantially as the RE element varies from Tb to Ho at a given temperature below ~30 K and the magnetization change becomes steepest around the transition temperature in the Ho containing alloy, indicating an enhancement of the interaction between the 3*d* electrons in transition metal and the 4*f* electrons in the heavy RE elements. From the magnetization behavior, a large -ΔS_M resulting from the acutest orientation of magnetic moments should be expected. For each alloy, obvious divergence between M_{FC} and M_{ZFC} branches occurs around a cusp of the M_{ZFC} curve, showing a typical SG like behavior. Defined as the temperature where the cusp appears, the spin freezing temperatures (T_f) are 55, 37 and 21 K for $Gd_{25}RE_{25}Co_{25}Al_{25}$ HE alloys with RE = Tb, Dy and Ho, respectively. Due to the absence of orbital angular momentum in Gd, the ferromagnetism instead of SG state was usually observed in many Gd-based amorphous alloys [6,9,17]. On the contrary, in other RE-based alloys, the long-range ferromagnetic order was broken by the large random magnetic anisotropy (RMA) and spins are strongly oriented along their anisotropy axes under local anisotropy field at low temperature, which causes the formation of complex ground states with a random orientation of magnetic moments and magnetic irreversibility [11,13,25]. In $Gd_{25}RE_{25}Co_{25}Al_{25}$ glassy alloys with RE = Tb, Dy and Ho whose orbital moments are unequal to zero, the RMA arising from the interactions between the local electrostatic fields and the random atomic arrangements of 4*f* atoms plays a significant role, leading to a SG like behavior [11–13,26]. Ascribed to the inversely magnetization caused by the remnant magnetic field in the sample chamber, negative starting values in the M_{ZFC} curves can be seen in Fig. 2. Calculated from the differentiation of M_{FC} curves, Curie temperatures (T_C) corresponding to the minimum of d*M*/d*T* are determined to be 73, 60 and 50 K for the HE alloys with RE = Tb, Dy and Ho, respectively, as marked by arrows in the inset of Fig. 2.

Based on the Rudermann-Kittel-Kasuya-Yosida (RKKY) indirect interaction theory, a positive relationship between T_C and de Gennes factor (*G*) was proposed for RE alloys ($T_C \propto I(0)G$, where $I(0)$ is the indirect exchange integral.) [16,27]. The *G* can be expressed as: $G = J(J+1)(g-1)^2$, where *J* represents the total orbital quantum number (*J* = 6, 7.5 and 8 for RE = Tb, Dy and Ho, respectively), and *g* represents the gyromagnetic ratio given by $g = 1 + [J(J+1) + S(S+1) - L(L+1)]/2J(J+1)$, where *S* represents the spin quantum number, and *L* represents the orbital angular momentum quantum number (*S* = 3, 2.5, 2 and *L* = 3, 5, 6 for Tb, Dy, Ho elements, respectively)) [16,28]. The *G* values of Tb, Dy, and Ho calculated theoretically are 10.5, 7.1 and 4.5, respectively. This is consistent with the experiment results that the T_C of the alloy system decreases gradually as the RE element changes from Tb to Ho. The T_C versus *G* is presented in Fig. 3 for the studied glassy alloys, as well as some other typical HE metallic glasses for comparison [10,16]. It can be seen that, the slope of this quaternary system is larger than the slopes for pentabasic alloys, indicating larger $I(0)$ and stronger RKKY interactions in these quaternary alloys. As these exchange

Table 1
The glass transition temperature (T_g), crystallization temperature (T_x), supercooled liquid region ($\Delta T_x = T_x - T_g$), Curie temperature (T_C), spin freezing temperature (T_f), configurational entropy (ΔS_{config}), maximum magnetic entropy change (ΔS_M^{max}), full width at half maximum magnetic entropy change (δT_{FWHM}), and refrigeration capacity (RC) under a magnetic field of 5 T of $Gd_{25}RE_{25}Co_{25}Al_{25}$ (RE = Tb, Dy, Ho) glassy alloys, together with other HE alloys reported recently.

Composition	T_g (K)	T_x (K)	ΔT_x (K)	T_C (K)	T_f (K)	$-\Delta S_M^{max}$ (J kg^{-1}K^{-1})	δT_{FWHM} (K)	RC (J kg^{-1})	ΔS_{config} (J mol^{-1}K^{-1})	Ref.
$Gd_{25}Tb_{25}Co_{25}Al_{25}$	612	659	47	73	55	8.88	65	577	11.53	This work
$Gd_{25}Dy_{25}Co_{25}Al_{25}$	627	669	42	60	37	8.72	65	567	11.53	This work
$Gd_{25}Ho_{25}Co_{25}Al_{25}$	633	675	42	50	21	9.78	64	626	11.53	This work
$Er_{20}Dy_{20}Co_{20}Al_{20}Tb_{20}$	623	663	40	29	24	8.6	61	525	13.38	[10]
$Er_{20}Dy_{20}Co_{20}Al_{20}Tm_{20}$	645	690	45	13	11	11.9	34	405	13.38	[10]
$Gd_{20}Tb_{20}Dy_{20}Ni_{20}Al_{20}$	582	607	25	45	38	7.25	70	507	13.38	[16]
$Gd_{20}Tb_{20}Dy_{20}Co_{20}Al_{20}$	594	626	32	58	41	9.43	67	632	13.38	[16]
$Gd_{10}Tb_{10}Dy_{10}Ho_{10}Er_{10}$-$Y_{10}Ni_{10}Co_{10}Ag_{10}Al_{10}$	597	636	39	24	15	10.64	50	532	19.11	[36]

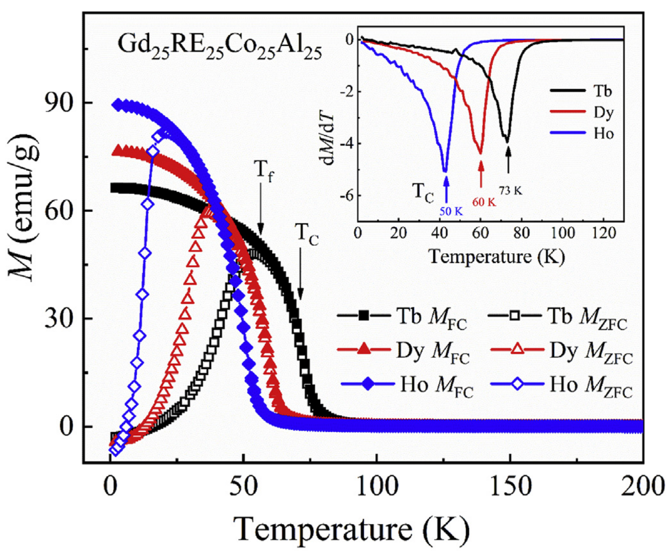

Fig. 2. Temperature dependence of M_{FC} and M_{ZFC} curves for the $Gd_{25}RE_{25}Co_{25}Al_{25}$ (RE = Tb, Dy, Ho) glassy alloys under an applied magnetic field of 200 Oe. The inset shows the dM/dT curves for the glassy ribbons.

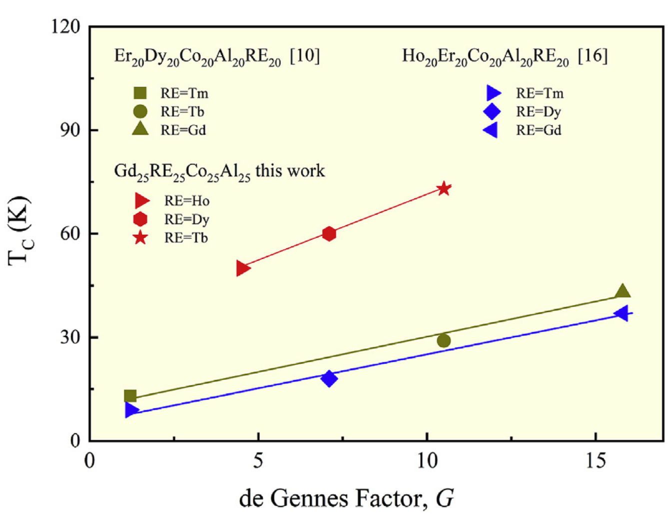

Fig. 3. Curie temperature T_C versus de Gennes Factor G for the glassy alloys in this work together with other reported high entropy metallic glasses.

interactions depend locally on the interatomic distances of RE elements and number of conduction electrons [27], a tunable transition temperature could be designed by adjusting the alloy composition with different RE substitution. And the G value should be a good guidance for estimating the T_C in compositions containing different RE elements. Additionally, the higher Gd (with G value of 15.8) content results in a higher T_C in these HE alloys compared to the pentabasic alloys shown in Fig. 3.

To characterize the critical dynamics of the SG transition, AC susceptibility measurements at different frequencies for $Gd_{25}RE_{25}Co_{25}Al_{25}$ HE glassy alloys were carried out. As shown in the insets of Fig. 4, serial susceptibility curves with sharp peaks can be observed in each alloy, meanwhile, the peak values shift to higher temperatures and decrease with increasing frequency. For a critical slowing down of the dynamics, the correlation length diverges at the transition temperature and the relaxation time ($\tau_{max} = 1/\omega$) obeys the power law as follows [29]:

$$\tau_{max} = \tau_0 \times \left(T_f / T_s - 1\right)^{-z\nu} \tag{1}$$

where T_s and $z\nu$ are the ideal freezing temperature and a critical exponent, respectively, τ_0 is related to the relaxation time of individual atomic magnetic moment. τ_0 and $z\nu$ were reported to be ~10^{-10}-10^{-13} s and 4–13 [29], respectively, for antitype SGs. It can be seen from Fig. 4 that the experimental data were fitted with Eq. (1) very well for each alloy, demonstrating a critical divergence. The fitting results for $Gd_{25}RE_{25}Co_{25}Al_{25}$ glassy alloys are: with RE = Tb, τ_0 = ~10^{-12} s, T_s = 69.9 K, $z\nu$ = 4.3, with RE = Dy, τ_0 = ~10^{-12} s, T_s = 55.7 K, $z\nu$ = 5.9, and with RE = Ho, τ_0 = ~10^{-13} s, T_s = 47.1 K, $z\nu$ = 4.8, respectively. Both the τ_0 and $z\nu$ values locate in the range of conventional SGs. It can be found that the HE glassy alloys in this work show obviously smaller τ_0 values than the Dy- (on the order of 10^{-6}) or Ho- (on the order of 10^{-9}) based metallic glasses [26,30]. The increasing microscopic characteristic time τ_0 is reported in accordance with the increasing ratio of RMA to the exchange interaction [26,29,30]. The τ_0 value of the alloy with RE = Ho is smaller than those of alloys with RE = Tb and Dy, suggesting a smaller RMA in the Ho containing alloy. The $z\nu$ values of these alloys are comparable with the value obtained from Ogielski's simulation for Ising SGs [31]. In addition, the T_s decreases as RE element changes from Tb to Ho, which is corresponding to the trend observed in the DC magnetization curves.

To evaluate the MCE of the glassy alloys, isothermal magnetization of the $Gd_{25}RE_{25}Co_{25}Al_{25}$ ribbons with RE = Tb, Dy and Ho in a large temperature range were measured and plotted in Fig. 5(a–c), respectively. For each alloy, the magnetization of the sample rises abruptly and then slowly approaches to saturation at temperatures below T_C, showing obvious ferromagnetic behavior. On the contrary, the magnetization curves gradually turn to straight lines at temperatures above T_C, confirming the ferromagnetic-paramagnetic transition. The intersection between the magnetization curves at 10 and 20 K can be attributed to the SG like

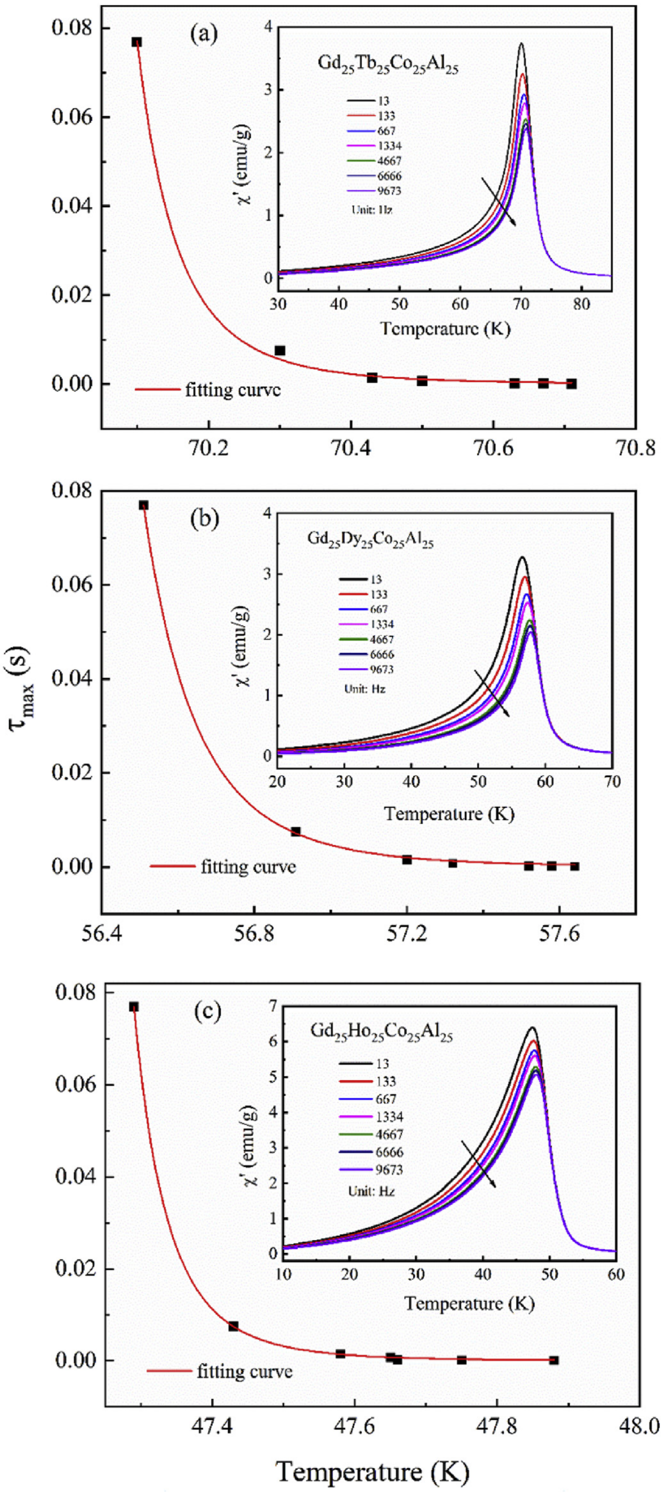

Fig. 4. The relaxation time τ_{max} versus temperature for $Gd_{25}RE_{25}Co_{25}Al_{25}$ glassy alloys with RE = Tb (a), Dy (b), and Ho (c). The insets are the χ' at frequencies ranging from 13 to 9673 Hz.

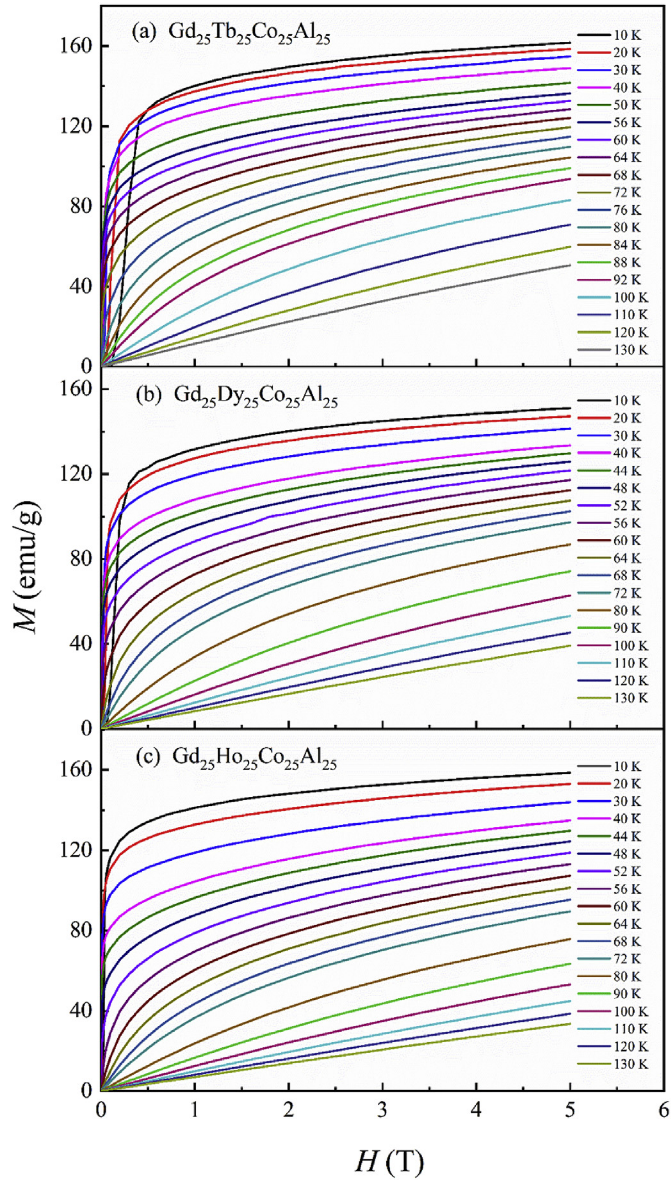

Fig. 5. Isothermal magnetization curves for $Gd_{25}RE_{25}Co_{25}Al_{25}$ glassy alloys with RE = Tb (a), Dy (b), and Ho (c) at the temperature range of 10–130 K.

magnetic behavior, which was also observed in the GdNiAl alloys [9]. Fig. 6(a–c) show the corresponding Arrott plots for $Gd_{25}RE_{25}Co_{25}Al_{25}$ HE alloys with RE = Tb, Dy and Ho, respectively, and the inserts show the magnified plots at 10, 20 and 30 K. According to Banerjee criterion [32], a magnetic transition is supposed to be a second order phase transition when the slopes of Arrott plots are positive, which usually implies a low hysteresis. Plots with positive slope can be observed in Fig. 6(a–c), demonstrating a second order magnetic phase transition in these HE glassy alloys.

The ΔS_M is considered as one of the main parameters to characterize the MCE of a magnetic refrigerant and can be evaluated from the isothermal magnetization curves. Fig. 7(a–c) display the temperature dependence of ΔS_M under different magnetic fields for $Gd_{25}RE_{25}Co_{25}Al_{25}$ glassy alloys with RE = Tb, Dy and Ho, respectively, which are calculated by integrating the Maxwell relation over the magnetic field [33]:

$$\Delta S_M(T,H) = S_M(T,H) - S_M(T,0) = \int_{H_0}^{H_{max}} \left(\frac{\partial M}{\partial T}\right) dH \qquad (2)$$

where H_{max} represents the maximum value of the magnetic field, and H_0 is defined to be 0 T in this work. The -ΔS_M increases with the increase of the applied magnetic field in the whole temperature

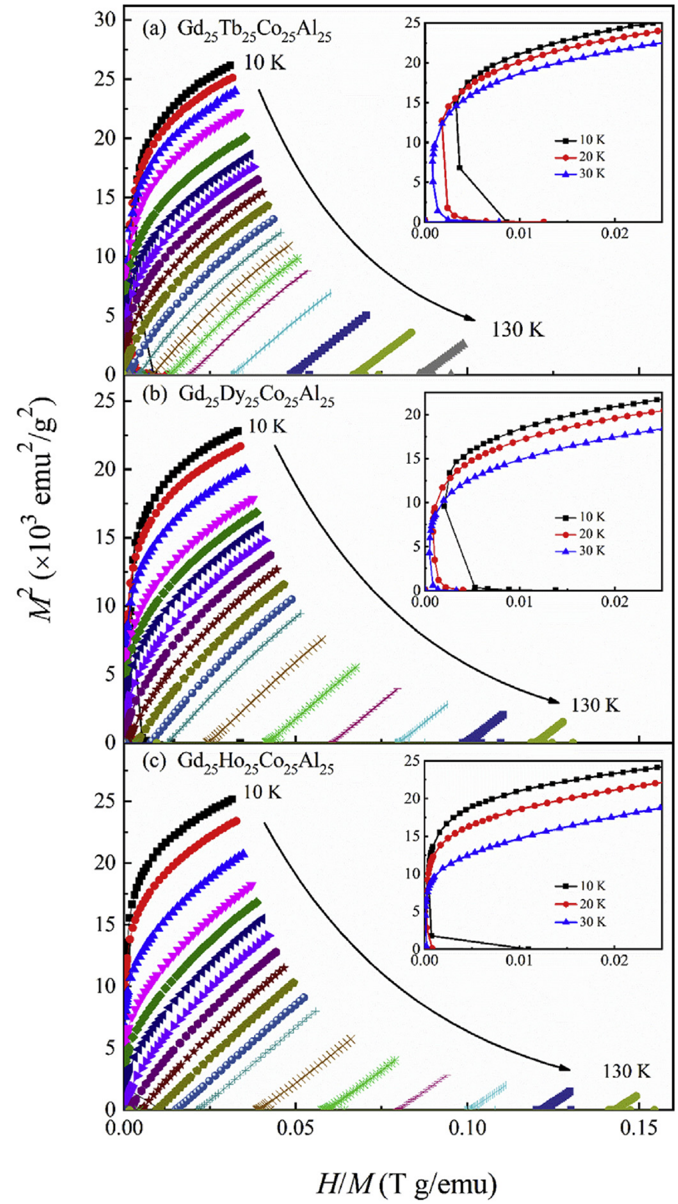

Fig. 6. Arrott plots for $Gd_{25}RE_{25}Co_{25}Al_{25}$ glassy alloys with RE = Tb (a), Dy (b), and Ho (c). The inserts are the magnified for 10 K, 20 K and 30 K, respectively.

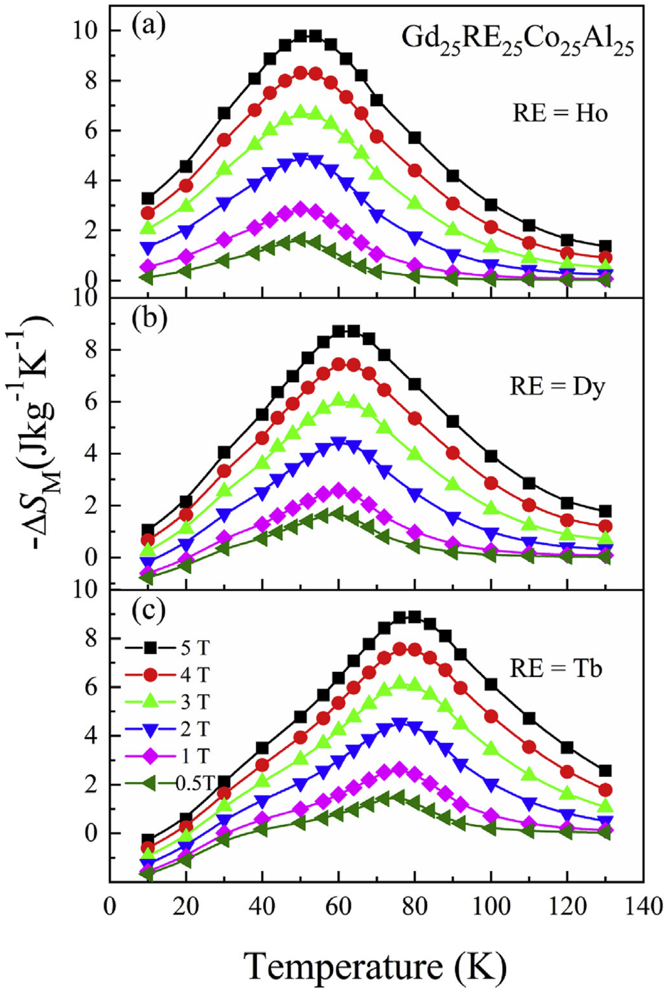

Fig. 7. Magnetic entropy change as a function of temperature under an applied magnetic field of 0.5, 1, 2, 3, 4 and 5 T for (a) $Gd_{25}Ho_{25}Co_{25}Al_{25}$, (b) $Gd_{25}Dy_{25}Co_{25}Al_{25}$, and (c) $Gd_{25}Tb_{25}Co_{25}Al_{25}$ HE glassy alloys.

range for each alloy, and can be understood by the larger change of magnetic order degree under higher applied magnetic field. It is worthy to note that the maximum of magnetic entropy change ($-\Delta S_M^{max}$) also shifts to higher temperature with increasing magnetic field, which should be interpreted by the change of the magnetic free energy. Generally, there is higher magnetic free energy in a paramagnetic state comparing with ferromagnetic state, and the existence of the paramagnetic phase in a system would lead to an increase of the free energy [34]. A higher applied magnetic field makes the alloy system more magnetic oriented and thus lower the free energy, resulting in a shift of the -ΔS_M^{max} to higher temperature. As illustrated in Fig. 7, the variation of ΔS_M with temperature can be explained as below. For each alloy, as temperature decreases to the temperature corresponding to the -ΔS_M^{max}, the exchange interactions become stronger comparing with the thermal energy, leading to an increase in the magnetization and ΔS_M. Meanwhile, the RMA increases gradually and influences the spin structure, therefor slows down the spin flipping, then the RMA increases continuously and tends to a value that comparable with the exchange interactions, consequently, the ΔS_M decreases gradually from the temperature corresponding to the -ΔS_M^{max} to lower temperature [13]. Besides, irreversible positive ΔS_M is observed in $Gd_{25}Tb_{25}Co_{25}Al_{25}$ and $Gd_{25}Dy_{25}Co_{25}Al_{25}$ glassy alloys under different magnetic fields at very low temperatures, except in $Gd_{25}Ho_{25}Co_{25}Al_{25}$ glassy alloy. This should be attributed to the large RMA in Tb and Dy containing alloys which could be overcome in a higher magnetic field. Due to the small RMA in Ho containing alloy, positive ΔS_M was not observed in Fig. 7 (c) [12,13]. The values of -ΔS_M^{max} are evaluated to be 8.88, 8.72 and 9.78 J $kg^{-1}K^{-1}$ under an applied magnetic field of 5 T for $Gd_{25}RE_{25}Co_{25}Al_{25}$ glassy alloys with RE = Tb, Dy and Ho, respectively, indicating a tunable ΔS_M by substituting different RE elements. The large -ΔS_M^{max} value in these glassy alloys can be attributed to their high magnetic moments.

As another key parameter to evaluate the MCE of these glassy alloys, refrigeration capacity (*RC*) can be estimated using Gschneidner method [35]: $RC = -\Delta S_M^{max} \times \delta T_{FWHM}$, where δT_{FWHM} represents the full width at half -ΔS_M^{max}. Under an applied magnetic field of 5 T, *RC* values for compositions with RE = Tb, Dy and Ho are evaluated to be 577, 567 and 626 J kg^{-1}, respectively. The magnetocaloric properties for some typical HE glassy alloys are listed in Table 1, as well as their ΔS_{config} values. The quaternary

$Gd_{25}RE_{25}Co_{25}Al_{25}$ HE glassy alloys ($\Delta S_{config} = 11.53$) in this work exhibit large MCE, which is comparable with that of the other HE metallic glasses with higher rare earth content and larger ΔS_{config} [10,15,36]. With RE = Ho, the $Gd_{25}Ho_{25}Co_{25}Al_{25}$ glassy alloy exhibits the largest $-\Delta S_M^{max}$ and *RC* values among the three alloys in this work. The high *RC* should be attributed to the large ΔS_M and δT_{FWHM}, which is usually regarded as a result of the disordered atomic distribution in amorphous alloys. Cocktail effects in the HE alloys result in a composite effect on properties, wherein the interactions among the different elements themselves play an important role [18]. It is worth noting that the magnetic properties (e.g., T_f, T_C, $-\Delta S_M^{max}$, and *RC*) in the $Gd_{25}RE_{25}Co_{25}Al_{25}$ HE alloys can be gradually modulated by substituting different RE elements as listed in Table 1, suggesting the cocktail effect in these HE glassy alloys. Furthermore, the ΔS_M may be correlated with the ΔS_{config}, i.e., higher ΔS_{config} may contributes to a larger $-\Delta S_M^{max}$, but the exact correlation between the MCE and the ΔS_{config} in HE alloys should be further studied experimentally and theoretically in the future. For materials with a second order phase transition, the relationship between $-\Delta S_M$ and magnetic field can be expressed as a power law: $-\Delta S_M \propto H^n$ [37]. Fig. 8 shows the magnetic field dependence of $-\Delta S_M^{max}$ for $Gd_{25}RE_{25}Co_{25}Al_{25}$ (RE = Tb, Dy, Ho) alloys, and the inset displays the exponent *n* as a function of temperature. The *n* values obtained for $-\Delta S_M^{max}$ are 0.754, 0.735 and 0.765 for glassy alloys with RE = Tb, Dy and Ho, respectively, and are close to those of other amorphous alloys [4,5,37]. The larger exponent *n* for $-\Delta S_M^{max}$ than that of the mean-field theoretical predictions (2/3) can be attributed to a distribution of T_C [38], which originates from the local inhomogeneity (i.e. chemical short-range order) existent in these glassy alloys [39]. From the plots in the inset, exponent *n* values of the alloys were found ~2 in the paramagnetic range as a consequence of the Curie-Weiss law [37].

4. Conclusions

In summary, $Gd_{25}RE_{25}Co_{25}Al_{25}$ (RE = Tb, Dy, Ho) HE glassy alloys with distinct SG like behavior and large MCE were studied. The results can be concluded as follows:

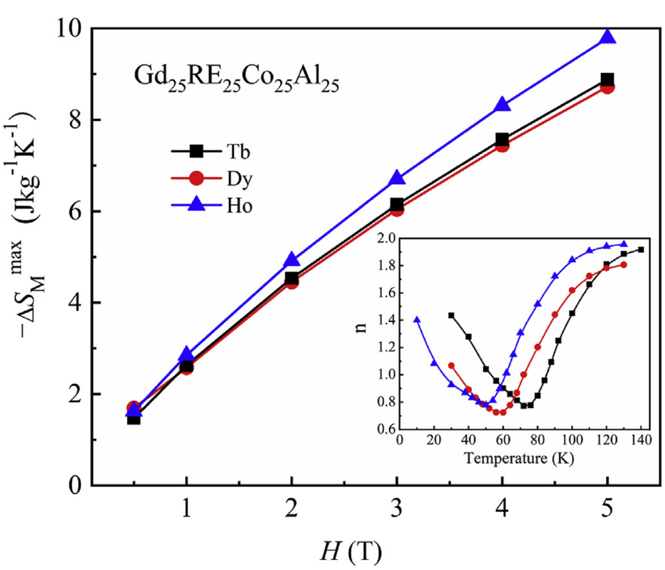

Fig. 8. Field dependence of the maximum magnetic entropy change and temperature dependence of *n* (the inset) for $Gd_{25}RE_{25}Co_{25}Al_{25}$ (RE = Tb, Dy, Ho) glassy alloys.

(1) Quaternary $Gd_{25}RE_{25}Co_{25}Al_{25}$ (RE = Tb, Dy, Ho) HE glassy alloys were fabricated. With different RE substitution, the T_C of the alloys can be easily tuned from 50 to 73 K, which is consistent with the variation of the de Gennes factor.

(2) Distinct SG like behavior was observed in $Gd_{25}RE_{25}Co_{25}Al_{25}$ (RE = Tb, Dy, Ho) HE glassy alloys. These alloys show critical spin freezing dynamics around T_f, and the fitted τ_0 and exponent $z\nu$ values of the alloys locate in the range of conventional SGs. Compared with the other two alloys, $Gd_{25}Ho_{25}Co_{25}Al_{25}$ alloy shows the smallest τ_0 value, demonstrating the smallest RMA in the Ho containing alloy.

(3) Under a magnetic field of 5 T, $-\Delta S_M^{max}$ values of the alloys with RE = Tb, Dy and Ho are 8.88, 8.72 and 9.78 J kg^{-1}K^{-1}, respectively, and *RC* values for alloys with RE = Tb, Dy and Ho are 577, 567 and 626 J kg^{-1}, respectively. The large MCE, as well as the inherent amorphous nature make these HE glassy alloys, especially $Gd_{25}Ho_{25}Co_{25}Al_{25}$, promising candidates for refrigerant applications.

Acknowledgments

This work was supported by the National Natural Science Foundation of China (Grant Nos. 51631003 and 51471050), the Fundamental Research Funds for the Central Universities (Grant No. KYLX15_0121), and the Scientific Research Foundation of Graduate School of Southeast University (Grant No. YBJJ1673).

References

[1] O. Tegus, E. Brück, L. Zhang, Dagula, K.H.J. Buschow, F.R.D. Boer, Magnetic-phase transitions and magnetocaloric effects, Phys. B Condens. Matter 319 (2002) 174–192.
[2] V. Provenzano, A.J. Shapiro, R.D. Shull, Reduction of hysteresis losses in the magnetic refrigerant $Gd_5Ge_2Si_2$ by the addition of iron, Nature 429 (2004) 853–857.
[3] J. Liu, T. Gottschall, K.P. Skokov, J.D. Moore, O. Gutfleisc, Giant magnetocaloric effect driven by structural transitions, Nat. Mater. 11 (2012) 620–626.
[4] W.M. Yang, J.T. Huo, H.S. Liu, J.W. Li, L.J. Song, Q. Li, L. Xue, B.L. Shen, A. Inoue, Extraordinary magnetocaloric effect of Fe-based bulk glassy rods by combining fluxing treatment and J-quenching technique, J. Alloys Compd. 684 (2016) 29–33.
[5] P. Yu, N.Z. Zhang, Y.T. Cui, L. Wen, Z.Y. Zeng, L. Xia, Achieving an enhanced magneto-caloric effect by melt spinning a $Gd_{55}Co_{25}Al_{20}$ bulk metallic glass into amorphous ribbons, J. Alloys Compd. 655 (2016) 353–356.
[6] P. Yu, N.Z. Zhang, Y.T. Cui, Z.M. Wu, L. Wen, Z.Y. Zeng, L. Xia, Achieving better magneto-caloric effect near room temperature in amorphous $Gd_{50}Co_{50}$ alloy by minor Zn addition, J. Non-Cryst. Solids 434 (2016) 36–40.
[7] H.F. Belliveau, Y.Y. Yu, Y. Luo, F.X. Qin, H. Wang, H.X. Shen, J.F. Sun, S.C. Yu, H. Srikanth, M.H. Phan, Improving mechanical and magnetocaloric responses of amorphous melt-extracted Gd-based microwires via nanocrystallization, J. Alloys Compd. 692 (2017) 658–664.
[8] V. Provenzano, R.D. Shull, G. Kletetschka, P.E. Stutzman, $Gd_{90}Co_{2.5}Fe_{7.5}$ alloy displaying enhanced magnetocaloric properties, J. Alloys Compd. 622 (2015) 1061–1067.
[9] F. Yuan, J. Du, B.L. Shen, Controllable spin-glass behavior and large magnetocaloric effect in Gd-Ni-Al bulk metallic glasses, Appl. Phys. Lett. 101 (2012), 032405.
[10] J. Li, L. Xue, W.M. Yang, C.C. Yuan, J.T. Huo, B.L. Shen, Distinct spin glass behavior and excellent magnetocaloric effect in $Er_{20}Dy_{20}Co_{20}Al_{20}RE_{20}$ (RE= Gd, Tb and Tm) high-entropy bulk metallic glasses, Intermetallics 96 (2018) 90–93.
[11] J. Du, Q. Zheng, E. Brück, K.H.J. Buschow, W.B. Cui, W.J. Feng, Spin-glass behavior and magnetocaloric effect in Tb-based bulk metallic glass, J. Magn. Magn. Mater. 321 (2009) 413–417.
[12] Q. Luo, B. Schwarz, N. Mattern, J. Eckert, Irreversible and reversible magnetic entropy change in a Dy-based bulk metallic glass, Intermetallics 30 (2012) 76–79.
[13] Q. Luo, B. Schwarz, N. Mattern, J. Eckert, Giant irreversible positive to large reversible negative magnetic entropy change evolution in Tb-based bulk metallic glass, Phys. Rev. B 82 (2010), 024204.
[14] Y.K. Zhang, B.J. Yang, G. Wilde, Magnetic properties and magnetocaloric effect in ternary REAgAl (RE=Er and Ho) intermetallic compounds, J. Alloys Compd. 619 (2015) 12–15.
[15] J.T. Huo, L.S. Huo, H. Men, X.M. Wang, A. Inoue, J.Q. Wang, The magnetocaloric effect of Gd-Tb-Dy-Al-M (M= Fe, Co and Ni) high-entropy bulk metallic glasses, Intermetallics 58 (2015) 31–35.

[16] J.T. Huo, L.S. Huo, J.W. Li, H. Men, X.M. Wang, A. Inoue, High-entropy bulk metallic glasses as promising magnetic refrigerants, J. Appl. Phys. 117 (2015), 073902.
[17] H.X. Shen, D.W. Xing, J.L. Sánchez Llamazares, C.F. Sánchez-Valdés, H. Belliveau, H. Wang, F.X. Qin, Y.F. Liu, J.F. Sun, H. Srikanth, M.H. Phan, Enhanced refrigerant capacity in Gd-Al-Co microwires with a biphase nanocrystalline/amorphous structure, Appl. Phys. Lett. 108 (2016), 092403.
[18] J.W. Yeh, Recent progress in high-entropy alloys, Ann. Chim. - Sci. Mater. 31 (2006) 633–648.
[19] J. Kim, H.S. Oh, J. Kim, C.W. Ryu, G.W. Lee, H.J. Chang, E.S. Park, Utilization of high entropy alloy characteristics in Er-Gd-Y-Al-Co high entropy bulk metallic glass, Acta Mater. 155 (2018) 350–361.
[20] Y. Zhang, T.T. Zuo, Z. Tang, M.C. Gao, K.A. Dahmen, P.K. Liaw, Z.P. Lu, Microstructures and properties of high-entropy alloys, Prog. Mater. Sci. 61 (2014) 1–93.
[21] C. Chen, K. Wong, R.P. Krishnan, Z.F. Lei, D.H. Yu, Z.P. Lu, S.M. Chathoth, Highly collective atomic transport mechanism in high-entropy glass-forming metallic liquids, J. Mater. Sci. Technol. 35 (2019) 44–47.
[22] Z. Zhang, M.M. Mao, J.W. Wang, B. Gludovatz, Z. Zhang, S.X. Mao, E.P. George, Q. Yu, R.O. Ritchie, Nanoscale origins of the damage tolerance of the high-entropy alloy CrMnFeCoNi, Nat. Commun. 6 (2015).
[23] Y.X. Ye, C.Z. Liu, H. Wang, T.G. Nieh, Friction and wear behavior of a single-phase equiatomic TiZrHfNb high-entropy alloy studied using a nanoscratch technique, Acta Mater. 147 (2018) 78–89.
[24] Y. Yuan, Y. Wu, X. Tong, H. Zhang, H. Wang, X.J. Liu, L. Ma, H.L. Suo, Z.P. Lu, Rare-earth high-entropy alloys with giant magnetocaloric effect, Acta Mater. 125 (2017) 481–489.
[25] C. Jayaprakash, S. Kirkpatrick, Random anisotropy models in the Ising limit, Phys. Rev. B 21 (1980) 4072.
[26] Q. Luo, D.Q. Zhao, M.X. Pan, W.H. Wang, Critical and slow dynamics in a bulk metallic glass exhibiting strong random magnetic anisotropy, Appl. Phys. Lett. 92 (2008), 011923.
[27] K.N.R. Taylor, M.I. Darby, Physics of Rare Earth Solids, Chapman and Hall, London, 1972.
[28] J.K.A. Gschneidner, A.O. Pecharsky, V.K. Pecharsky, in: R.G. Ross Jr. (Ed.), Cryocoolers 12, Springer Science+Business Media, NewYork, 2003, p. 457.
[29] K. Binder, A.P. Young, Spin-glasses-experimental facts, theoretical concepts, and open question, Rev. Mod. Phys. 58 (1986) 801–976.
[30] Q. Luo, B. Schwarz, N. Mattern, J. Eckert, Magnetic ordering and slow dynamics in a Ho-based bulk metallic glass with moderate random magnetic anisotropy, J. Appl. Phys. 109 (2011) 113904.
[31] A.T. Ogielski, Dynamics of three-dimensional Ising spin glasses in thermal equilibrium, Phys. Rev. B 32 (1985) 7384–7398.
[32] S.K. Banerjee, On a generalized approach to first and second order magnetic transitions, Phys. Lett. 12 (1964) 16–17.
[33] T. Hashimoto, T. Numasawa, M. Shino, T. Okada, Magnetic refrigeration in the temperature range from 10 K to room temperature: the ferromagnetic refrigerants, Cryogenics 21 (1981) 647–653.
[34] Y.S. Liu, J.C. Zhang, Y.Q. Wang, Y.Y. Zhu, Z.L. Yang, J. Chen, S.X. Cao, Weak exchange effect and large refrigerant capacity in a bulk metallic glass $Gd_{0.32}Tb_{0.26}Co_{0.20}Al_{0.22}$, Appl. Phys. Lett. 94 (2009) 112507.
[35] K.A. Gschneidner Jr., V.K. Pecharsky, Magnetocaloric materials, Annu. Rev. Mater. Sci. 30 (2000) 387–429.
[36] J.T. Huo, J.Q. Wang, W.H. Wang, Denary high entropy metallic glass with large magnetocaloric effect, J. Alloys Compd. 776 (2019) 202–206.
[37] V. Franco, J.S. Blázquez, A. Conde, Field dependence of the magnetocaloric effect in materials with a second order phase transition: a master curve for the magnetic entropy change, Appl. Phys. Lett. 89 (2006) 222512.
[38] V. Franco, A. Conde, V. Provenzano, R.D. Shull, Scaling analysis of the magnetocaloric effect in $Gd_5Si_2Ge_{1.9}X_{0.1}$ (X=Al, Cu, Ga, Mn, Fe, Co), J. Magn. Magn. Mater. 322 (2010) 218–223.
[39] X.M. Huang, X.D. Wang, Y. He, Q.P. Cao, J.Z. Jiang, Are there two glass transitions in Fe-M-Y-B (M = Mo, W, Nb)bulk metallic glasses? Scripta Mater. 60 (2009) 152–155.